



ELSEVIER

Journal of Membrane Science 140 (1998) 185–194

journal of  
MEMBRANE  
SCIENCE

## Effects of precipitation conditions on the membrane morphology and permeation characteristics

Dong-Tsamn Lin<sup>a</sup>, Liao-Ping Cheng<sup>b</sup>, Yu-Jung Kang<sup>c</sup>, Leo-Wang Chen<sup>d</sup>, Tai-Horng Young<sup>c,\*</sup>

<sup>a</sup>Department of Laboratory Medicine, College of Medicine, National Taiwan University, Taipei 10016, Taiwan, ROC

<sup>b</sup>Department of Chemical Engineering, Tamkang University, Taipei, Taiwan, ROC

<sup>c</sup>Center for Biomedical Engineering, College of Medicine, National Taiwan University, Taipei 10016, Taiwan, ROC

<sup>d</sup>Department of Chemical Engineering, National Taiwan University, Taipei, Taiwan, ROC

Received 24 February 1997; received in revised form 13 October 1997; accepted 16 October 1997

### Abstract

The permeability and permselectivity of asymmetric and particulate membranes towards glucose and proteins of various molecular sizes were studied. It was found that the skin layer of asymmetric membranes was permeable to glucose and insulin but effectively prevent the permeation of immunoglobulins. This result parallels our interest for the development of artificial pancreas. It was also found that skinless particulate membranes exhibited not only high permeation rates with respect to albumin and immunoglobulins but also good selectivity between these components. Thus, particulate membranes has the potential to be used in separating albumin from immunoglobulins for treating disorders related to immunoglobulin abnormalities. © 1998 Elsevier Science B.V.

**Keywords:** Asymmetric membranes; Particulate membranes; Glucose; Insulin; Albumin; Immunoglobulins

### 1. Introduction

During the past four decades, membrane separation process has experienced a notable growth in different phases of biomedical industry. Various novel membranes have been tailored to fulfill specific purposes and many of them have been commercialized, e.g., hemodialysis, controlled release, sterilization of heat-sensitive material, etc. The effectiveness of a membrane is often determined by its permeability and permselectivity with respect to the target components.

For instance, only small molecules (e.g., uric acid and creatinine) can penetrate hemodialysis membranes. In the development of artificial pancreas [1–10], proliferating investigations have been performed to integrate the islets of Langerhans into synthetic membranes, which can then be used to treat the type I diabetes mellitus. In such cases, the membrane is required to be permeable towards glucose and insulin. Yet, it must be absolutely impermeable to immunoglobulins and lymphocytes. In case that a membrane is to be employed in plasma fractionation for the treatment of immunologically related symptoms (e.g., abnormal immunoglobulins G, M (IgG or IgM) or immune complexes) [11–14], it has to be permselective toward albumin and immunoglobulins.

\*Corresponding author. Fax: 886-2-3940049, E-mail: [thyong@ha.mc.ntu.edu.tw](mailto:thyong@ha.mc.ntu.edu.tw)

Direct immersion–precipitation [15] is the process widely used to manufacture porous membranes, in which a polymer solution is immersed without evaporation into a bath of nonsolvent. At some stage, precipitation (sometimes recognized as liquid–liquid demixing, phase inversion, crystallization, or some combinations in the literature) occurs leading to the formation of a porous solid film. The structures of the formed membranes are very complex and are dependent upon the composition of coagulation bath [16–18]. In this study, two types of membranes were synthesized: particulate and traditional asymmetric membranes. There are several possible mechanisms for the formation of particles in the membrane. When the polymer concentration in the casting solution is lower than the critical point of binodal, particles are generated by the nucleation and growth of the polymer-rich phase resulted from liquid–liquid demixing [18,19]. Another possible origin of nodules is spinodal demixing [20]. It has also been proposed that crystallization of polymer is responsible for the formation of particles [21–24]. However, consensus has not yet been reached among membranologists regarding the formation mechanism of these particles. The particulate membranes were skinless and had open continuous pores between particles whereas the asymmetric membranes were generally skinned and had independent pores. Permeation of glucose and various proteins through the formed membranes were examined using plasma obtained from both healthy donor and systemic lupus erythematosus patients. We seek to find the relation between morphology and permeation properties of these membranes and ultimately the possibility of applying these membranes to various biomedical applications.

## 2. Materials and methods

### 2.1. Materials

The membrane materials used in this study were poly(ethylene-co-vinyl alcohol) (EVAL, E105A containing ca. 56 mole% vinyl alcohol, Kuraray, Japan), Nylon-610 (Ultramid S3, BASF) and poly(vinylidene fluoride) (PVDF, Kynar 740, Elf Ato Chem). All polymers were obtained from commercial sources and used as received. Dimethyl sulfoxide (DMSO),

*N,N*-dimethylformamide (DMF) and 1-octanol were purchased from Nacalai Tesque (Kyoto, Japan, extra pure reagent grade) and used as received to prepare membranes. Water was double distilled and deionized before use. Glucose (molecular weight = 180 Da, Sigma), insulin (molecular weight about 5,800 Da, nominal activity = 28 IU/mg; Sigma), bovine serum albumin (BSA, molecular weight about 67 kDa, fraction V, containing more than 99% monomeric albumin, Sigma), and human immunoglobulin G (IgG, molecular weight about 150 kDa, Sigma) were dissolved in phosphate buffer solution (PBS, pH = 7.4, Boehringer Ingelheim, Germany) to make feed solutions for permeability measurements.

### 2.2. Membrane preparation

Both asymmetric and particulate membranes were made by the immersion–precipitation method. An appropriate amount of polymer was dissolved in solvent to form a 25 wt% dope solution. Using an auto-coater, this dope was spread uniformly on a glass plate to form a 100  $\mu\text{m}$  film, which was immediately immersed into a coagulation bath maintained at 25°C for at least 30 min. During this period of time, precipitation occurs and the dope becomes a white solid laminate. Following Young and Chen's method [25], EVAL were precipitated into various asymmetric structures using coagulation baths that contain different amount of solvent (DMSO) and nonsolvent (water). The compositions of these coagulation baths are summarized in Table 1. Particulate membranes were made from three polymers, namely, EVAL, Nylon-610 and PVDF. Nylon-610 is made into a particulate morphology which is readily wetted by water. Although PVDF membranes are skinless, they

Table 1  
Preparation condition of asymmetric membranes (temp. of casting solution and coagulation bath: 25°C)

Membrane	Coagulation bath: DMSO/H <sub>2</sub> O
G1	0/1
G2	1/4
G3	2/3
G4	1/1
G5	2/1
G6	3/1

Table 2  
Preparation condition of particulate membranes (temp. of casting solution and coagulation bath: 25°C)

Membrane	Polymer/Solvent/Nonsolvent
P1	EVAL/DMSO/1-Octanol
P2	Nylon-610/DMF/1-Octanol
P3	PVDF/DMF/1-Octanol

are in fact hydrophobic and can not be wetted by water. EVAL contains hydrophilic vinyl alcohol segments and hydrophobic ethylene segments. Its wettability is intermediate of Nylon-610 and PVDF membranes. The preparation conditions for these particulate membranes are shown in Table 2. The non-solvent for these polymers is 1-octanol. It is very interesting that even though these polymers have rather different chemical properties, they all form membranes with particulate morphology as they are precipitated from 1-octanol [26–28].

The morphologies of different faces of the membranes were examined using a scanning electron microscope (SEM). The membranes were freeze-dried, then frozen in liquid nitrogen and fractured to expose the cross-sectional areas. The dried sample were gold coated and viewed with an SEM (S-800, Hitachi, Japan) at 20 kV.

### 2.3. Permeability measurements

The permeation by diffusion of various solutes (i.e., glucose, insulin, BSA, and human IgG) through the formed membranes were studied at 37°C. The concentrations of these solutions were 180 mg/dl for glucose, 400  $\mu$ U/ml for insulin, 3.5 g/dl for BSA, and 2 mg/ml for IgG, respectively. The diffusion experiments were carried out in a dual-chamber, well-stirred diffusion cell with a volume of 3.5 ml for each chamber. The membranes with an effective permeation area equal to 0.64 cm<sup>2</sup> were sandwiched in between the chambers. Vigorous agitation were employed, the speed of which was ca. 600 rpm, using independently controlled magnetic stirrers for both chambers.

The donor side of the diffusion cell was filled with PBS containing solute molecules and the receptor side was filled only with PBS. At selected intervals of time,

equal amount of samples (either 40 or 100  $\mu$ l) were taken from both compartments for subsequent examinations. Glucose and insulin concentrations were analyzed using a glucose analyzer and an enzyme immunoassay (Medgenix, Belgium), respectively. Concentrations of BSA and IgG were measured by a UV spectrophotometer at 280 nm.

### 2.4. Determination of mass transfer coefficients

The mass balance equation that describes the evolution of solute concentration in the receptor chamber is given by

$$V \frac{dC_r}{dt} = \frac{A}{L} D (C_d - C_r) \quad (1)$$

where  $C_d$  and  $C_r$  are concentrations of the solute in the donor and receptor chambers, respectively.  $A$  is the effective transport area for the solute,  $L$  is the thickness of the membrane,  $V$  is the volume of each chamber and  $D$  is the solute diffusion coefficient in membrane. Eq. (1) can be solved analytically to give

$$\ln \left[ \frac{(C_d - C_r)_t}{(C_d - C_r)_0} \right] = -2 \frac{DA}{LV} t \quad (2)$$

where  $(C_d - C_r)_0$  and  $(C_d - C_r)_t$  refers, respectively, to the initial concentration difference and that at time  $t$ . Linear regression analysis of the above equation gives the slope  $2DA/LV$ , from which the membrane diffusive permeability ( $D/L$ , mass transfer coefficient) can be calculated. In these experiments, the mass transfer boundary layer resistance near the membrane surface was found to be much smaller than the membrane resistance according to the procedure proposed by Smith et al. [29] and Colton [30], and accounted for less than 1.5% of total mass transfer resistance. Therefore, the diffusion resistance at the liquid–membrane interface can be neglected when the permeation test was performed with sufficient mixing.

### 2.5. Water flux and plasma ultrafiltration

Pure water flux and plasma ultrafiltration were determined using a 25 mm dia. Amicon Stirred Ultrafiltration Cell (Model 8010) at a stirring speed of 600 rpm. The transmembrane pressure was equal to 0.5 kgf/cm<sup>2</sup> connected to a compressed nitrogen gas source. The plasma used in this work was extracted

from human blood of healthy donors and systemic lupus erythematosus patients. This blood was centrifuged (Beckman CS-15R, USA) at 4500 rpm to obtain the supernatant plasma. All filtration experiments were carried out at room temperature ( $23 \pm 2^\circ\text{C}$ ). After the permeate flux reaches a stable constant value (ca. 50 min after operation), the filtrate samples were collected for 3 h for subsequent analysis. The albumin and the IgG content were measured by using the Array Protein System (Beckman) and the Nephelometer-Analyser (Behring), respectively. It is interesting to notice that abnormal plasma composition (especially, high IgG count in the plasma) was observed for all of the patients with systemic lupus erythematosus. In addition, a 100 ppm of blue dextran (average molecular weight = 2,000 kDa, Sigma) solution was filtered to check whether the membrane was defected. All tested membranes were found to reject the passage of this blue dextran.

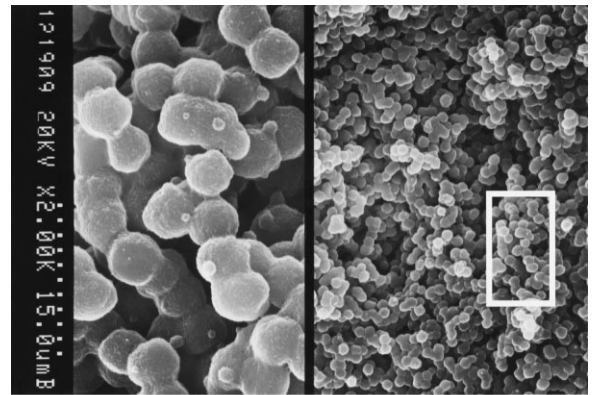
### 3. Results and discussion

#### 3.1. Morphologies of asymmetric and particulate membranes

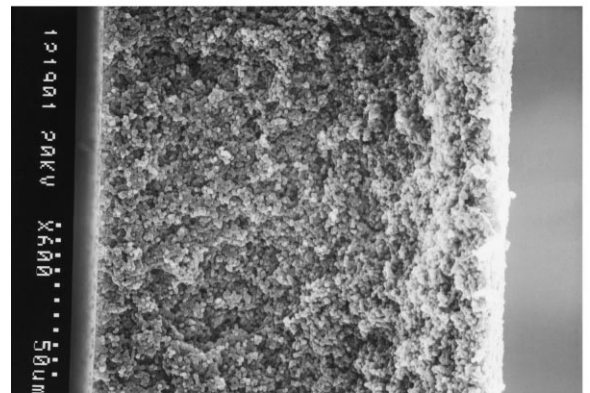
The SEM photomicrographs of membranes G1–G6 were given in a previous report (see Figs. 5–10 of Ref. [25]). Membranes G1–G4 exhibited a typical asymmetric structure composed of a thin and dense skin layer and a porous bulk that contains independent finger-like cavities enclosed in a porous solid matrix. The skin layer is responsible for the permeation or rejection of solutes whereas the porous bulk acts as a mechanical support. Membrane structure may be regulated by a variety of methods, one of which is to adjust the concentration of the coagulation bath. As shown by Young and Chen [25], the skin layer became less dense and the finger-like macrovoids became less evident, as the DMSO (solvent) content in the coagulation bath was increased (i.e., the bath becomes “softer” with respect to polymer precipitation). The macrovoids may sometimes be eliminated, if the bath contains a significant amount of solvent. Membranes G5 and G6 are such instances, as can be seen from the SEM (Figs. 9 and 10 of Ref. [25]) that the macrovoids of these membranes are absent and that the surface layers become somewhat porous. Young and Chen

have rationalized the formation mechanism for these structures [17,25]. Since the skin layer dictates the permselectivity of a membrane, it is very important to have a strict control of the membrane formation conditions, in case that solute molecules of different sizes are to be fractionated in a filtration process.

The morphologies of the top surface and cross-section of the particulate membranes, P1–P3, are shown in Figs. 1–3 Unlike other asymmetric membranes (G1–G6), these membranes are uniform and skinless characterized by a packed bed of nearly equal-diameter particles that fuse together at the interfaces. Because all pores are interconnected, these membranes exhibit the so-called “co-continuous”

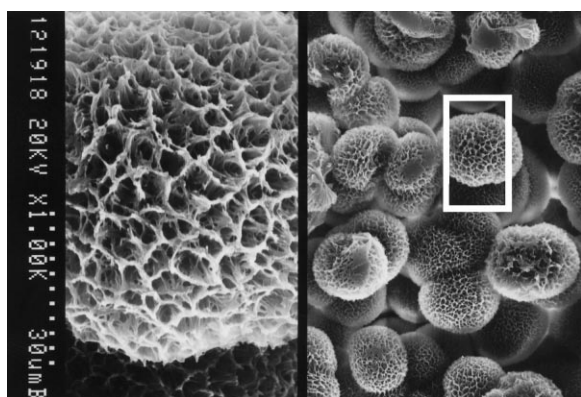


(a)

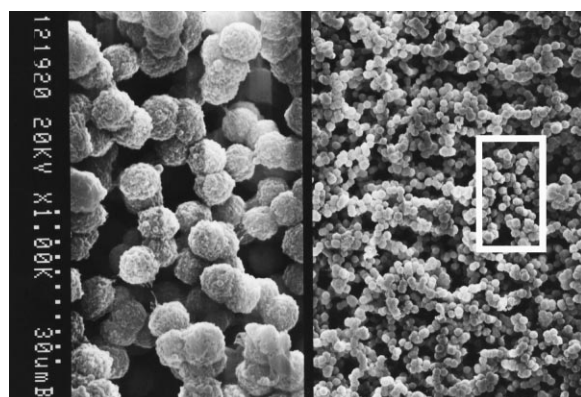


(b)

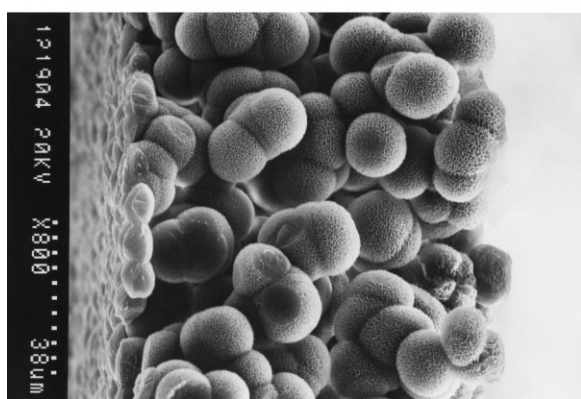
Fig. 1. SEM photomicrographs of membrane P1: (a) top surface, (b) cross section.



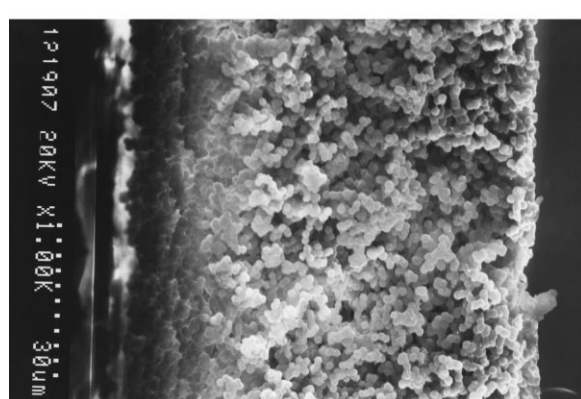
(a)



(a)



(b)



(b)

Fig. 2. SEM photomicrographs of membrane P2: (a) top surface, (b) cross section.

Fig. 3. SEM photomicrographs of membrane P3: (a) top surface, (b) cross section.

structure. The pore size and therefore the filtration capability of these membranes is closely related to the size of the particles. As shown in Figs. 1–3, Nylon-610 precipitates from 1-octanol into very large particles (ca. 8  $\mu\text{m}$  dia. in membrane P2) whereas EVAL and PVDF membranes have much smaller particles (ca. 1  $\mu\text{m}$  dia. in membranes P1 and P3).

### 3.2. Permeation studies of single component

Permeation measurements of solutions containing only one kind of solute molecule were carried out for various membranes in a dual-chamber diffusion cell. The concentration of solute in both chambers were

monitored. In Fig. 4, the measured data for glucose permeation are presented in the form conforming to Eq. (2). From the slope of each best-fitted line, mass transfer coefficient ( $D/L$ ) was calculated for each membrane. These results are shown in Table 3. It is observed that all membranes are permeable to glucose with a mass transfer coefficient on the order of  $10^{-4}$  cm/s. For the permeation of other solutes (insulin, albumin and IgG), likewise, a linear relationship was obtained complying with Eq. (2). The calculated mass transfer coefficients for these cases are summarized in Table 3. For each membrane, as is anticipated, the mass transfer coefficient is smaller for larger solute molecules. Several asymmetric membranes (G2, G4

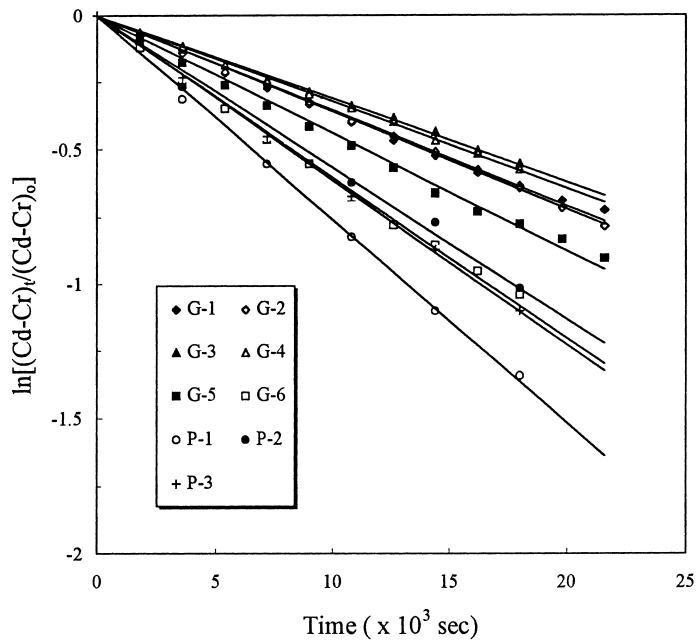


Fig. 4. Time dependent permeation of glucose through various membranes.

Table 3  
Mass transfer coefficients for various solutes (cm/sec)

Membrane	Glucose	Insulin	Albumin	IgG
G1	$9.65 \times 10^{-5}$	— <sup>a</sup>	—	—
G2	$9.70 \times 10^{-5}$	$2.50 \times 10^{-5}$	$7.11 \times 10^{-7}$	ND <sup>b</sup>
G3	$8.48 \times 10^{-5}$	—	—	—
G4	$8.77 \times 10^{-5}$	$2.51 \times 10^{-5}$	$9.77 \times 10^{-7}$	ND
G5	$1.19 \times 10^{-4}$	—	—	—
G6	$1.64 \times 10^{-4}$	$3.23 \times 10^{-5}$	$1.13 \times 10^{-6}$	ND
P1	$2.06 \times 10^{-4}$	$3.72 \times 10^{-5}$	$2.10 \times 10^{-6}$	$1.19 \times 10^{-6}$
P2	$1.53 \times 10^{-4}$	$3.61 \times 10^{-5}$	$3.28 \times 10^{-6}$	$1.37 \times 10^{-6}$
P3	$1.67 \times 10^{-4}$	$3.55 \times 10^{-5}$	$1.44 \times 10^{-5}$	$2.09 \times 10^{-6}$

<sup>a</sup>Not tested. <sup>b</sup>ND=not detectable after 24 h permeation.

and G6) were found to reject completely IgG for the period of 24 h (the detection limit of UV spectrophotometer is calibrated to be  $0.005 \mu\text{g/dl}$  of IgG). Although it is possible that IgG is able to diffuse across these membranes in longer operation times [31], a 24 h experiment is long enough to evaluate preliminarily whether a membrane has the potential to separate various proteins before proteins denature. Table 3 indicates that the mass transfer coefficients of the particulate membranes (P1–P3) are roughly twice larger than those of the asymmetric membranes,

except for membrane G6 which has a porous top surface and an open cellular structure in the interior. This suggests that the dense skin of the asymmetric membranes offers the major resistance against solute transportation. In addition, because these asymmetric membranes are permeable to albumin while rejecting IgG, the pores in the skin layer can be considered between the dimension of albumin (67 kDa) and IgG (150 kDa).

If a membrane is to be implanted as a part of the artificial pancreas system, it must allow rapid permea-

tion of glucose and insulin so as to provide therapeutic benefits. Ward et al. reported recently the diffusive permeability of  $5.5 \times 10^{-5}$  cm/s for glucose through polyurethane membranes [6]. For commercial membranes, the glucose mass transfer coefficient of the Vitafiber cell was found to be  $3.67 \times 10^{-5}$  cm/s on the average and the Amicon and polyacrylonitrile membranes have similar diffusive permeabilities [32]. The experimental data indicates that membrane G2 appears to have a higher diffusive permeability with respect to glucose (ca.  $9.70 \times 10^{-5}$  cm/s) for use in an artificial pancreas. On the other hand, the membrane has to be permselective to prevent the influx of IgG and other larger antibodies which cause rejection of the islets inside the membranes. For the membranes shown in Table 3, it appears that all of the asymmetric membranes are suitable choices to be built into the artificial pancreas system; in particular G6, since it is not only impermeable to IgG but also has the largest mass transfer coefficients both with respect to glucose and insulin.

Table 3 shows that skinless particulate membranes, in general, exhibit a higher solute permeation rate than asymmetric ones. For particulate membranes, an ordinary diffusion path for solutes is the tortuous but continuous void space between fused particles (Note: one other path is the nano-pores within the particle. This point is discussed in a separate publication [33]). Since the diameter of this path is relatively large, large solute molecules, such as IgG, can pass it at a reasonable speed. In contrast, asymmetric membranes have a skin layer as being a region with very small pore size that provides an effective diffusion barrier for solutes. In Table 4, water flux data are given at transmembrane pressure equal to  $0.5 \text{ kgf/cm}^2$  for

both types of membranes. The data for membrane P3 is not included because its water flux is higher than the measurable range of our apparatus. As is anticipated, particulate membranes have water fluxes significantly higher than those of the asymmetric ones. However, because of their low permselectivity towards IgG, these particulate membranes should not be used in an artificial pancreas system.

### 3.3. Solute rejection during filtration of plasma

In order to examine the permeability of one type of solute in the presence of the others and also to know the performance of the membranes in realistic conditions, filtration experiments were carried out using human plasma as the feed in a dead-end filtration. Feed and filtrate samples were analyzed to yield the data of total protein concentrations, sieving coefficients, and selectivity of albumin relative to IgG for various membranes. These results are shown in Table 5(a) for the normal plasma (from healthy donors) cases and in Table 5(b) for the abnormal plasma (from patients) cases. From Table 5(a), it can be seen that IgG could not penetrate asymmetric membranes G1–G4, but could pass through membranes G5 and G6 to a significant degree. This is different from the results obtained from the single-component diffusion experiments (see Table 3) which indicate that all asymmetric membranes are impermeable to IgG. One possible explanation for this observation is that in a pressure driven filtration process, molecules are compressed to become more compact so as to enter the membrane skin layer more easily [34,35]. Also, because membranes G5 and G6 were prepared from very soft baths, their skins are not dense and thus are permeable to large molecules such as IgG. Table 5(a) shows that albumin are undetectable in the permeate for membranes G1–G3. This should be attributed to the resolution of the instrument. Analyzing the plasma proteins is far more difficult than that for single protein. The lower measurable limits in this study are 22.2 mg/dl and 170 mg/dl for albumin and IgG, respectively.

As far as particulate membranes (P1 and P2) are concerned, more albumin and IgG passed through them than the asymmetric ones, as shown in Table 5(a). Membrane P2 has a higher albumin sieving coefficient than membrane P1; its capability to

Table 4  
Water flux with transmembrane pressure  $0.5 \text{ kgf/cm}^2$

Membrane	Flux (l/h $\text{m}^2$ atm)
G1	18
G2	20
G3	58
G4	62
G5	90
G6	76
P1	140
P2	110

Table 5  
Filtrate concentrations, sieving coefficient and selectivity for plasma ultrafiltration

Membrane	Filtrate analysis			Sieving coefficient ( $S$ ) <sup>c</sup>		Selectivity <sup>d</sup>
	TP <sup>a</sup> (g/dl)	Alb <sup>b</sup> (g/dl)	IgG (mg/dl)	Alb	IgG	
(a) Normal plasma						
Feed: TP=6.4 g/dl, Alb=3.3 g/dl, IgG=1100 mg/dl						
G1	ND <sup>c</sup>	ND	ND	ND	ND	—
G2	ND	ND	ND	ND	ND	—
G3	ND	ND	ND	ND	ND	—
G4	0.6	0.4	ND	0.121	ND	—
G5	2.7	1.5	315	0.455	0.286	1.591
G6	2.6	1.6	316	0.485	0.287	1.670
P1	3.5	2.0	366	0.606	0.333	1.820
P2	4.6	2.3	844	0.670	0.767	0.874
(b) Abnormal plasma						
Feed: TP=16.5 g/dl, Alb=2.1 g/dl, IgG=14800 mg/dl						
G2	ND	ND	ND	ND	ND	—
G4	1.1	0.1	900	0.048	0.061	0.787
G6	3.2	0.3	2050	0.143	0.139	1.029
P1	7.5	1.0	6100	0.476	0.412	1.155
P2	14.6	1.9	12400	0.905	0.838	1.080

<sup>a</sup>TP = Total Protein; <sup>b</sup>Alb = Albumin; <sup>c</sup>Sieving coefficient ( $S$ ) =  $C_{out}/C_{in}$ ; <sup>d</sup>Selectivity =  $S_{Alb}/S_{IgG}$ ; <sup>e</sup>ND= not detectable.

separate albumin from IgG is, however, much lower than membrane P1. The selectivity (albumin/IgG=1.820) of membrane P1 is the highest among all membranes in normal plasma filtration. The G5 and G6 membranes have good selectivity (albumin/IgG) as well, but their fluxes and sieving coefficients toward albumin are too low. In order to achieve an effective plasma fractionation, membranes are required to reject as much as possible IgG while at the same time recover most albumin in the plasma. This suggests that membrane P1 is better than G5 and G6, and even better than the commercial membranes [11]. Therefore, membrane P1 is an alternative to patients with certain classes of autoimmune diseases that are currently treated by plasma exchange.

Comparison of Table 5(a) and Table 5(b) indicates that filtration of abnormal plasma yields results largely consistent with those from normal plasma filtration. Again, membrane P1 has the highest albumin/IgG selectivity ( $S=1.155$ ) among all membranes. Its value is, however, significantly lower than that for normal plasma ( $S=1.82$ ). This may be attributed to the high IgG concentration in the abnormal plasma, in which case some smaller pores of the membrane are likely to be plugged by IgG aggregates. In addition, the aggre-

gation of IgG, especially for the high IgG concentration, at the upstream membrane surface that causes concentration polarization also may reduce the permeation of albumin. For these reasons, the albumin sieving coefficient is decreased from 0.606 for normal plasma filtration to the current value of 0.476. Similar situations are observed for asymmetric membranes, G4 and G6, whose pores are smaller than those of membrane P1. Table 5 indicates that the albumin permeation has reduced considerably (to ca. 1/3 of the value for normal plasma) for these membranes. Contrary to these cases, the albumin sieving coefficient of membrane P2 is higher in abnormal plasma filtration. Because the pores of membrane P2 are very large (Fig. 2), it is impossible to plug them even in concentrated IgG solutions. (The increase in albumin sieving coefficient is still unexplainable at present.) This paper places emphasis upon discussing the performances of asymmetric and particulate membranes towards various proteins. No attempt is made to describe the mechanism that governs multicomponent mass transfer in actual plasma ultrafiltration processes. However, enthusiastic investigations are currently undergoing on subjects, such as the effect of protein concentration, the effect of concentration



polarization, the effects of size and packing pattern of particles in particulate membranes, the effect of transmembrane pressure upon permeation of various species during filtration, etc.

#### 4. Conclusion

The structures of these membranes were found to affect significantly their permeability and selectivity towards glucose and various proteins in human plasma. In order to work as an immunoprotective barrier for the artificial pancreas, the membrane has to have a skin which is dense enough to prevent inward diffusion of IgG and other larger antibodies. On the other hand, the skin has to be somewhat porous to admit fast transportation of glucose and insulin. The results of current work indicate that this can be achieved by adjusting the “softness” of the coagulation bath during membrane formation. In addition, experimental evidences point out that some asymmetric EVAL membranes and particulate membranes (EVAL and Nylon-610) are potential candidates for plasma proteins fractionations. Especially, the particulate membranes which exhibit high permeation rates and good selectivity with respect to various species in plasma. This encourages us to continue our pursuing for a membrane capable of separating effectively albumin from immunoglobulins in fractionation operations.

#### Acknowledgements

The authors thank the National Science Council of the Republic of China for their financial support, project number: NSC 86-2314-B-002-173 and NSC 86-2216-E002-003.

#### References

- [1] F. Lim, A.M. Sun, Microencapsulated islets as bioartificial endocrine pancreas, *Science* 210 (1980) 908–910.
- [2] J.J. Altman, A. Houlbert, P. Callard, P. McMillan, B.A. Solomon, J. Rosen, P.M. Galetti, Long term plasma glucose normalization in experimental diabetic rats with macroencapsulated implants of benign human insulinomas, *Diabetes* 35 (1986) 625–633.
- [3] K. Inoue, T. Fujisato, Y.J. Gu, K. Burczak, S. Sumi, M. Kogire, T. Tobe, K. Uchida, I. Nakai, S. Maetani, Y. Ikada, Experimental hybrid islet transplantation: application of polyvinyl membrane for entrapment islets, *Pancreas* 7 (1992) 562–568.
- [4] K. Burczak, T. Fujisato, M. Hatadaand, Y. Ikada, Protein permeation through poly(vinyl alcohol) hydrogel membranes, *Biomaterials* 15 (1994) 231–237.
- [5] R.P. Lanza, A.M. Beyer, W.L. Chick, Xenogenic humoral responses to islets transplanted in biohybrid diffusion chambers, *Transplantation* 57 (1994) 1371–1375.
- [6] R.S. Ward, K.A. White, C.A. Wolcott, A.Y. Wang, R.W. Kuhn, J.E. Taylor, J.K. John, Development of a hybrid artificial pancreas with a dense polyurethane membrane, *ASAIO J.* 39 (1993) 261–267.
- [7] L. Kessler, M. Pinget, M. Aprahamian, D. Poinot, M. Keipes, C. Damge, Diffusion properties of an artificial membrane used for Langerhans islets encapsulation: interest of an in vitro test, *Transplant. Proc.* 24 (1992) 953–954.
- [8] T. Zekorn, R.G. Bretzel, U. Siebers, W. Doppl, M. Renardy, P. Zschocke, H. Planck, K. Federlin, Protein coat causes improved insulin diffusion through membranes for immunoisolated islet transplantation. Improved islet survival by pretreatment of membrane and islets, *Transplant. Proc.* 22 (1990) 867–869.
- [9] L. Kessler, G. Legeay, C. Jesser, C. Damge, M. Pinget, Influence of corona surface treatment on the properties of an artificial membrane used for Langerhans islets encapsulation: permeability and biocompatibility studies, *Biomaterials* 16 (1995) 185–191.
- [10] T.H. Young, N.K. Yao, R.F. Chang, L.W. Chen, Evaluation of asymmetric poly(vinyl alcohol) membranes for use in the artificial islets, *Biomaterials* 17 (1996) 2139–2145.
- [11] M. Zborowski, P.S. Malchesky, Pore size and temperature effects in membrane separation of albumin from immunoglobulins, *ASAIO Trans.* 36 (1990) 730–733.
- [12] C. Charcosset, M.Y. Jaffrin, L. Ding, Time and pressure dependence of sieving coefficients during membrane plasma fractionation, *ASAIO Trans.* 36 (1990) 594–597.
- [13] M. Zborowski, P.S. Malchesky, Y. Nose, Temperature dependent protein removal by large pore membrane filtration, *ASAIO Trans.* 35 (1989) 572–575.
- [14] T. Horiuchi, P.S. Malchesky, M. Usami, M. Emura, Y. Nose, Effect of plasma solute–membrane interaction on mean pore diameter, *ASAIO Trans.* 32 (1986) 429–434.
- [15] R.E. Kesting, *Synthetic Polymeric Membranes*, Wiley, New York, 1985.
- [16] T.H. Young, L.W. Chen, Roles of bimolecular interaction and relative diffusion rate in membrane structure control, *J. Membr. Sci.* 83 (1993) 153–166.
- [17] T.H. Young, L.W. Chen, Pore formation mechanism of membranes from phase inversion process, *Desalination* 103 (1995) 233–247.
- [18] T.H. Young, L.W. Chen, L.P. Cheng, Membranes with a microparticulate morphology, *Polymer* 37 (1996) 1305–1310.
- [19] K. Kamide, S. Manabe, in: D.R. Lloyd. (Ed.), *Material Science of Synthetic Membranes*, American Chemical Society, Washington D.C., pp. 197–228, 1985.

- [20] S.P. Nunes, T. Inoue, Evidence for spinodal decomposition and nucleation and growth mechanisms during membrane formation, *J. Membr. Sci.* 111 (1996) 93–103.
- [21] A.M.W. Bulte, B. Folkers, M.H.V. Mulder, C.A. Smolders, Membranes of semicrystalline aliphatic polyamide nylon 4,6: formation by diffusion-induced phase separation, *J. Apply. Polym. Sci.* 50 (1993) 13–26.
- [22] L.P. Cheng, A.W. Dwan, C.C. Gryte, Membrane formation by isothermal precipitation in polyamide–formic acid–water systems I. Description of membrane morphology, *J. Polym. Sci. Polym. Phys.* 33 (1995) 211–222.
- [23] L.P. Cheng, A.W. Dwan, C.C. Gryte, Membrane formation by isothermal precipitation in polyamide–formic acid–water systems II. Precipitation dynamics, *J. Polym. Sci. Polym. Phys.* 33 (1995) 223–235.
- [24] T.H. Young, J.Y. Lai, W.M. Yu, L.P. Cheng, Equilibrium phase behavior of the membrane forming water–DMSO–EVAL copolymer system, *J. Membr. Sci.* 128 (1997) 55–65.
- [25] T.H. Young, L.W. Chen, A two step mechanism of diffusion-controlled ethylene vinyl alcohol membrane formation, *J. Membr. Sci.* 57 (1991) 69–81.
- [26] L. Broens, D.M. Koenhen, C.A. Smolders, On the mechanism of formation of asymmetric ultra- and hyper-filtration membranes, *Desalination* 22 (1977) 205–219.
- [27] J.G. Wijmans, H.J.J. Rutten, C.A. Smolders, Phase separation phenomena in solutions of poly(2,6-dimethyl-1,4-phenylene-oxide) in mixtures of trichloroethylene, 1-octanol, and methanol: relationship to membrane formation, *J. Polym. Sci. Polym. Phys.* 23 (1985) 1941–1955.
- [28] W.R. Burghardt, L. Yilmaz, A.J. McHugh, Glass transition, crystallization and thermoreversible gelation in ternary PPO solution; relationship to asymmetric formation, *Polymer* 28 (1987) 2085–2092.
- [29] K.A. Smith, C.K. Colton, E.W. Merrill, L.B. Evans, Convective transport in a batch dialyzer. Determination of the true membrane permeability from a single measurement, *AIChE Symp. Ser.* 64 (1968) 45.
- [30] C.K. Colton, Permeability and transport studies in batch and flow dialyzers with applications to hemodialysis, Ph.D. Dissertation, M.I.T., Mass., USA, 1969.
- [31] C.K. Colton, E.S. Avgoustiniatos, Bioengineering in development of the hybrid artificial pancreas, *J. Biomech. Eng.* 113 (1991) 152–170.
- [32] M.Y. Jaffrin, G. Reach, D. Notelet, Analysis of ultrafiltration and mass transfer in a bioartificial pancreas, *J. Biomech. Eng.* 110 (1988) 1–10.
- [33] L.P. Cheng, H.Y. Lin, L.W. Chen, T.H. Young, Solute rejection of dextran by EVAL membranes with asymmetric and particulate morphologies, *Polymer*, in press.
- [34] H. Balmann, R. Nobrega, Deformation of dextran molecules. Causes and consequences in ultrafiltration, *J. Membr. Sci.* 40 (1989) 311–327.
- [35] G. Schock, A. Miquel, Characterization of ultrafiltration membranes: Cutoff determination by gel permeation chromatography, *J. Membr. Sci.* 41 (1989) 55–67.